Diesel Substitution with Hydrogen for Marine Engines

Panagiotis Karvounis, Gerasimos Theotokatos

Maritime Safety Research Centre, Department of Naval Architecture, Ocean, and Marine Engineering, University of Strathclyde, Glasgow, Scotland, United Kingdom
* Corresponding Author panagiotis.karvounis@strath.ac.uk

Abstract

Zero-carbon fuels are expected to catalyse the decarbonisation of the maritime industry, with hydrogen being considered a long-term solution. This study aimed to investigate the feasibility of using hydrogen as a secondary fuel in marine diesel engines. A marine four-stroke engine with a nominal power output of 10.5 MW at 500 rpm was investigated, whereas the hydrogen injection at the engine port was considered. A CFD model was set up in CONVERGE for both diesel and the diesel-hydrogen operating modes to investigate the effects of 20% hydrogen fuel fraction (by energy) on engine performance, emissions, and combustion characteristics. This model was validated against experimental data for the diesel operating mode. Based on a parametric study, the mesh characteristics were selected to compromise between the prediction error and the computational effort. The impact of 20% hydrogen energy fraction on the heat release rate (HRR) and NO_x emissions is comparing with the diesel mode. The results demonstrate that despite the reduction in carbon emissions when using hydrogen, the NO_x emissions increase by 2.5 times, whereas the lower compression ratio allows for engine free-knock operation. This study contributes to the identification of efficient and reliable combustion conditions for diesel-hydrogen dual-fuel marine engines.

Keywords: CFD model, Hydrogen, Combustion, Marine engines, Decarbonisation.

1. INTRODUCTION

Hydrogen, as an environmentally friendly fuel, has emerged as a promising long-term solution for achieving sustainability goals and advancing decarbonisation efforts within the maritime industry [1]. Recent empirical studies have provided valuable insights into the feasibility of hydrogen-powered engines operating under real-world conditions [2]. These investigations underscore the techno-economic viability of adopting hydrogen-based propulsion systems, particularly when considering specific incentivisation mechanisms such as carbon taxation. However, the investigation of hydrogen combustion for marine compression ignition engines presents a range of challenges [3], which predominantly arise from the distinctive physical properties of hydrogen compared to conventional diesel fuels.

One notable difference is the elevated auto-ignition temperature of hydrogen, which necessitates the use of significantly higher compression ratios when employed as the primary fuel source [4]. Consequently, to address ignition-related issues, a dual-fuel operational strategy has been proposed [11]. In this approach, a fuel with a higher reactivity, typically diesel, is directly injected to initiate combustion. Most investigations of dual-fuel engines have considered the direct injection of diesel fuel close to the top dead centre (TDC). Other combustion methods include premixed combustion involving hydrogen injection into the port manifold, in-cylinder diesel injection, and diffusion combustion, which includes both diesel and hydrogen in-cylinder direct injection [5]. The former also involves low-pressure hydrogen injection during the compression stroke, whereas the latter considers high-pressure injection near TDC, each resulting in distinct effects on performance and emission parameters [6].

The literature lacks studies that examine the use of hydrogen in marine engines and hydrogen port injection in compression ignition engines. The latter has been identified as an attractive case for retrofitted marine engines and hence is expected to attract interest in the maritime sector [7].

This study aims to comparatively investigate the impact of hydrogen use in compression ignition marine engines by employing CFD modelling. The large marine four-stroke engine operation in the diesel and diesel-hydrogen dual fuel (DF) modes was simulated to reveal the effects of hydrogen use on the combustion, performance, and emissions parameters. This study contributes to the identification of settings that require optimisation in hydrogen fuelled marine dual-fuel engines.

2. METHODOLOGY

This study investigated a nine-cylinder marine four-stroke engine with 10.5 MW nominal power.

DOI: https://doi.org/10.59490/moses.2023.657

The engine bore and stroke were 460 and 580 mm, respectively, and the compression ratio was 14:1.

The CONVERGE CFD commercial code is used in this study. The methodological steps are illustrated in Fig. 1. The diesel mode operation, as well as the geometrical characteristics and settings of the engine, are first considered. A grid dependency study was conducted. The validation of the CFD model-derived results for the diesel mode is performed against datasets acquired from onboard experimental campaigns and manufacturers shop test trials. A comprehensive description of the data-acquisition process was reported by Stoumpos et al. [8].

The investigated case studies included baseline diesel mode operation (D) at a medium load. n-Heptane fuel was directly injected into the cylinder. The injection pressure was 1400 bar, and the injection start was 6ºCA BTDC. In the dual-fuel mode (DF), hydrogen is injected into the intake ports, and the hydrogen-air mixture at the inlet valve close (IVC) is considered fully premixed (hence homogeneous). Diesel fuel was injected using the same settings as the diesel mode.

To identify stable combustion conditions (knock free) in the DF mode, a set of parametric studies was conducted, including exhaust gas recirculation (EGR), diesel start of injection (SOI) retard, and compression ratio (CR) decrease. Following a parametric investigation (not reported herein for brevity), the CR of 11 (instead of 14 for the diesel mode) was identified to lead to knock-free combustion, although it was associated with lower engine efficiency. This parametric investigation yielded the operational parameters shown in Fig. 2. It is worth noting that an increased in-cylinder temperature at the IVC (compared with the diesel mode) is required for effective hydrogen combustion. Further investigation of optimal conditions is required so that the engine can operate in both diesel and dual-fuel modes with the same compression ratio.

Hydrogen requires specific storage conditions and is expected to occupy seven times the gross tank volume of conventional MGO fuels [18]. Considering this, along with the decarbonisation targets for shipping operations, it is expected that marine dual-fuel engines will be adopted with partial hydrogen fuel use. Hence, this study considers a 20% hydrogen energy fraction (HEF), defined by equation (1), to identify trade-offs between engine performance and emissions parameters.

$$HEF = \frac{m_{H_2} LHV_{H_2}}{(m_D LHV_D)+(m_{H_2} LHV_{H_2})} \quad (1)$$

where $m_{D,}$ m_{H2} denote the injected masses of diesel and hydrogen, respectively, and *LHV* is the lower heating value of these fuels.

Lastly, comparative evaluation is conducted between diesel and the dual-fuel modes.

Table 1 presents the physical properties of the diesel and hydrogen fuels. The high auto-ignition temperature of hydrogen poses challenges for its stable combustion in compression ignition engines.

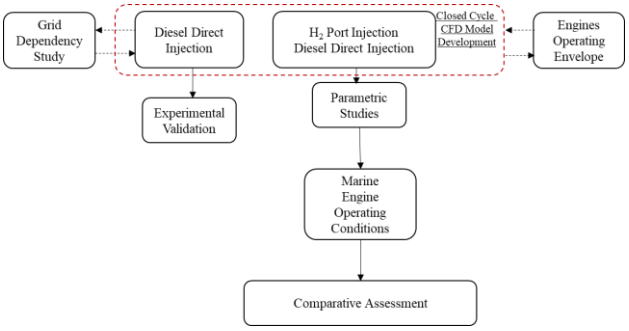

Figure 1. Methodology flowchart.

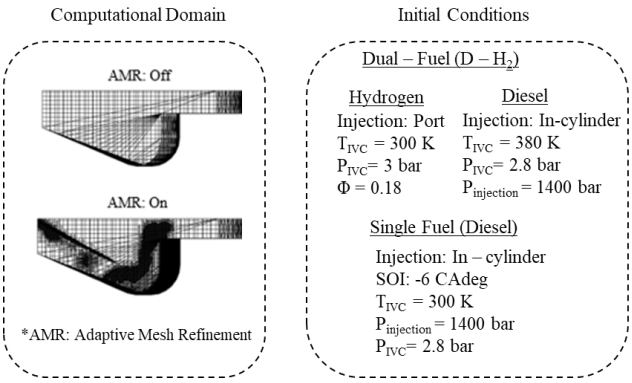

Figure 2. Computational domain and initial conditions of the CFD model.

Table 1. Fuel characteristics

Property	Diesel	Hydrogen
Density [kg/m^3] at 20ºC	847	0.083
Flash Point [ºC]	52	570
Auto-ignition temperature [ºC]	300	858
Viscosity [mPa] at 298.15 K	3.35	
Stoichiometric fuel–air ratio	0.069	0.029
Cetane number	55	–
Lower heating value [MJ/kg]	42.7	120
Latent heat of vaporisation [kJ/kg]	359	461
Laminar burning velocity [cm/s]	30	265–325

2.1 Computational Domain & Grid Sensitivity Study

A segment of one engine cylinder based on in-cylinder and diesel fuel injector (diesel jet deployment) symmetry was selected to reduce the computational cost of the model. The employed

computational domain is shown in Figure 2. The (sub)models employed to develop the CFD model are presented in Table 2.

Table 2. Simulation models.

Mechanisms	**Model**
Turbulence model	RANS k-ε
Droplet breakup model	KH-RT [13]
Spray/Wall interaction model	Han [14]
Droplets collision model	Nordin [15]
NO_x mechanism	Extended Zeldovich [16]
Reaction mechanism - Diesel	Rahimi [17]

A grid sensitivity analysis was performed to compromise between accuracy and computational time. The grid characteristics are presented in Table 3. For all grids, adaptive mesh refinement was used in conjunction with fixed embedding within the injector area to achieve higher resolution. Fig. 3 shows the in-cylinder pressure variations for the three grids. The G-1 grid was selected because it led to smaller errors (considering the measured in-cylinder pressure).

Table 3. Computational grid characteristics.

Parameter	**G3**	**G2**	**G1**
Element size [mm]	0.01	0.005	0.002
Maximum cells number (at TDC)	19242	153940	2460000
Error at Pmax (%)	2	0.8	0.3
Solution duration [h]	6	14	55

3. RESULTS

Fig. 4 shows the measured and derived in-cylinder pressure and heat release variations for the diesel mode. Slight deviations were observed between the measurements and CFD predictions. The estimated error for the in-cylinder peak pressure is approximately 1%, whereas the crank angle at the peak pressure exhibits an error of 6%.

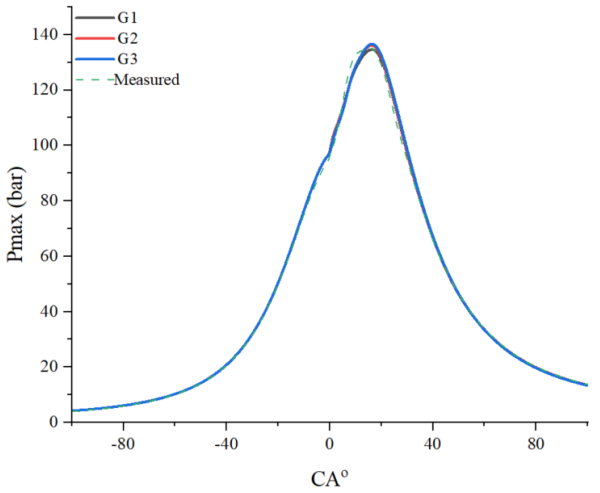

Figure 3. Derived in-cylinder pressure variations for different grids.

Figure 5 presents the measured and derived (by CFD model) NO concentration at the engine cylinder exhaust gas for the three engine loads. Errors of 3%, 8%, and 10% were estimated for 100%, 75%, and 50% loads, respectively, and the CFD model resulted in slight overprediction of the NO concentration. Furthermore, during the shop tests, NO was measured after the turbocharger turbine, whereas the simulated values corresponded to the cylinder at the exhaust valve opening, which also contributed to the deviations. Nevertheless, these errors are considered acceptable; hence, it is inferred that the CFD model is validated for the engine diesel mode. The measured data for the hydrogen fuelled mode were not available to further validate the CFD model. However, the developed model adequately represents the trade-offs for engine performance and emission parameters.

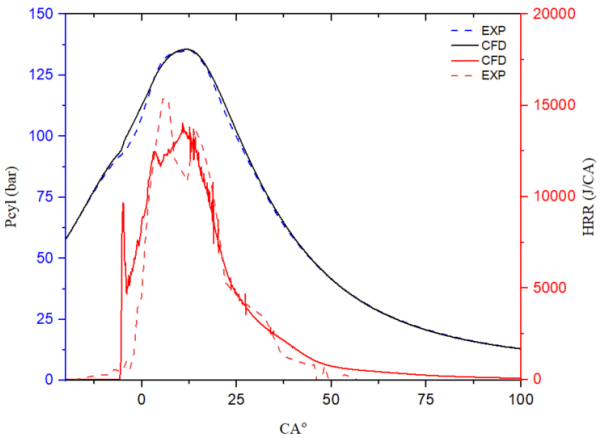

Figure 4. In-cylinder pressure and HRR variations.

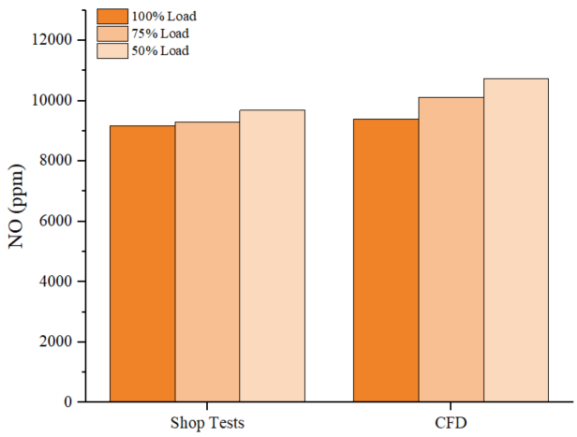

Figure 5. Measured and derived NO concentration.

Previous studies [9–10] have reported that hydrogen exhibits enhanced flame velocity compared to diesel, resulting in pronounced knocking phenomena within the engine, particularly at high loads, which leads to severe mechanical loading.

Fig. 6 shows the in-cylinder pressure variations in the diesel and DF modes. The maximum cylinder pressure was 136 bar and 100 bar for the D and DF cases, respectively, whereas the CA at Pmax shifted from 13.5 15.7ºCA ATDC.

Fig. 7 shows the derived heat release rate (HRR) for the diesel and dual-fuel modes. Owing to diesel dominance, the HRRs exhibited similar trends with some notable differences. The initial spike (3.7–0.3ºCA BTDC) is attributed to diesel premixed combustion. For the DF mode, the premixed hydrogen mixture along with the smaller injected diesel amount resulted in a slightly advanced start of combustion (SOC) at 5ºCA BTDC with a lower rate (HRR rate slope), leading to a lower spike peak value.

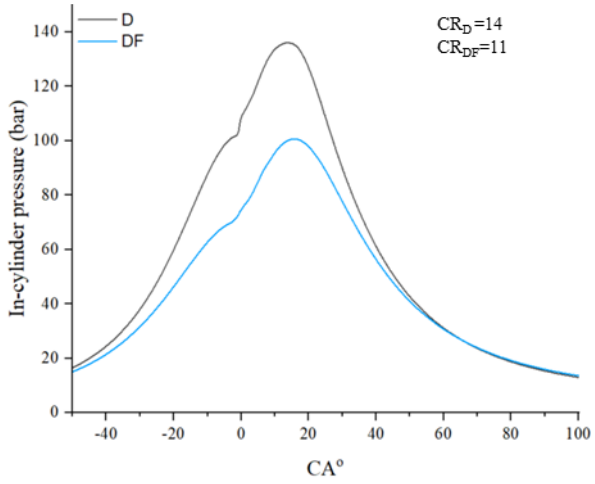

Figure 6. In-cylinder pressure variations for diesel and DF modes.

Following SOC, the hydrogen-air homogenous mixture burns under premixed conditions (flame front progressing in the combustion chamber). Simultaneously, the prepared diesel-air fuel mixture burns based on the diffusion combustion principles. Additionally, it is evident that in the DF mode, the combustion process in the 20–30ºCA ATDC evolves faster compared to the diesel mode (higher HRR), whereas most of the hydrogen (approximately 70% of the total amount) is burnt during this period. Notably, approximately 6% of the hydrogen remained unburnt.

The hydrogen-air mixture ignition occurs by the flame of diesel combustion at approximately 5ºCA ATDC, as can be observed in Fig. 11. From the variation in the hydrogen mass fraction (red line in Figure 7), the hydrogen combustion efficiency was estimated to be 93.7%. Between 0ºCA ATDC and 3ºCA ATDC, there was an increase in the mass fraction of hydrogen stemming from the diesel combustion products.

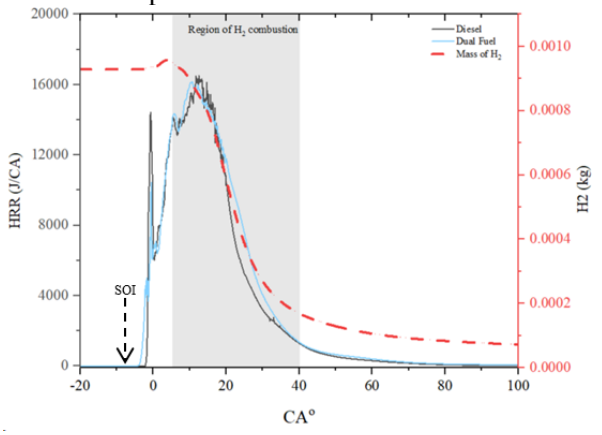

Figure 7. Heat release rates for the diesel and DF mode with 20% HEF. (b) represents the oxygen mass fraction at 5ºCA TDC where the hydrogen combustion initiates.

Fig. 8 illustrates the NO_x emissions in the diesel and dual-fuel modes. Hydrogen use requires a higher in-cylinder temperature to achieve satisfactory combustion efficiency. This leads to more favourable conditions for NO_x formation (compared to the diesel mode). The temperature threshold for thermal NO_x generation typically ranges between 1600 K and 1800 K. NO formation typically commences at 700 K. For the DF mode, a longer duration of residence above this temperature range leads to higher concentrations of thermal NO_x. To effectively reduce NO_x emissions, optimisation of the engine settings is required.

However, it is evident that the use of hydrogen primarily focuses on CO_2 reduction proportional to the HEF employed. The indicated thermal efficiency decreased from 43% in the D case to 41% in the DF case because of the increase in the heat transfer losses and CR reduction.

Potential pathways to mitigate NOx formation include the use of exhaust gas recirculation, engine setting optimisation, or the use of other lean combustion concepts.

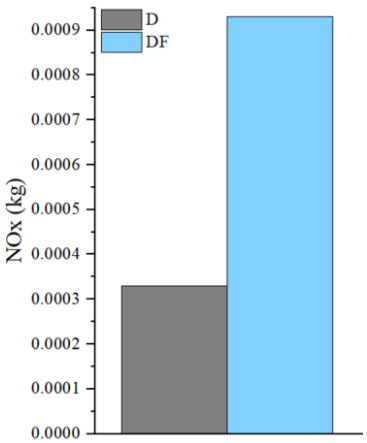

Figure 8. Derived NOx mass for the diesel mode and the DF mode with 20% HEF.

Fig. 9 shows the in-cylinder NO_x mass and temperature for different crank angles for the diesel and DF modes. As diesel is injected close to the TDC (6ºCA BTDC) and combustion occurs, the NO_x mass is zero as the temperature is not sufficiently high (>1800 K) to accommodate the oxidation of atmospheric nitrogen to NO and NO_2. At 3ºCA BTDC, the most volatile species of the diesel jet evaporated owing to the high-pressure, high-temperature regime.

The latter is also observed in Fig. 10, which shows the in-cylinder NOx mass and temperature variations for the diesel and DF modes. In the DF mode, the in-cylinder contents remained for a longer period at high temperatures (prolonged combustion duration), thus yielding a higher NOx concentration.

Fig. 11 shows the in-cylinder hydrogen mass fraction, which illustrates the progression of the hydrogen-air mixture combustion process. At 3ºCA BTDC, the hydrogen-air mixture combustion has not commenced, indicating that the heat release rate (HRR) spike (Fig. 7) is solely attributed to the injected diesel premixed combustion (prepared diesel-air mixture within the region 5–3.7ºCA BTDC). Notably, at 5ºCA ATDC, a considerable hydrogen fraction was noted in the near-wall region; this was attributed to the diesel combustion reactions leading to hydrogen production. The increased temperature in proximity to the diesel jet initiates hydrogen-air mixture combustion. The hydrogen mass fraction is considerably reduced in the period of 20–30ºCA ATDC with the flame front moving, whereas the remaining diesel fuel is burned via a diffusion combustion approach.

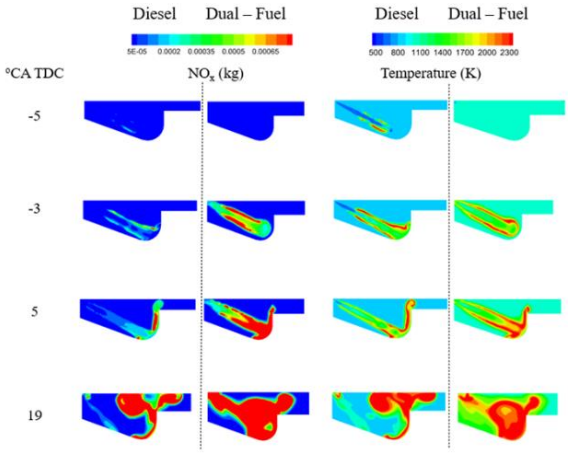

Figure 9. CFD contours of NOx concentration and in-cylinder temperature for single and dual – fuel operation

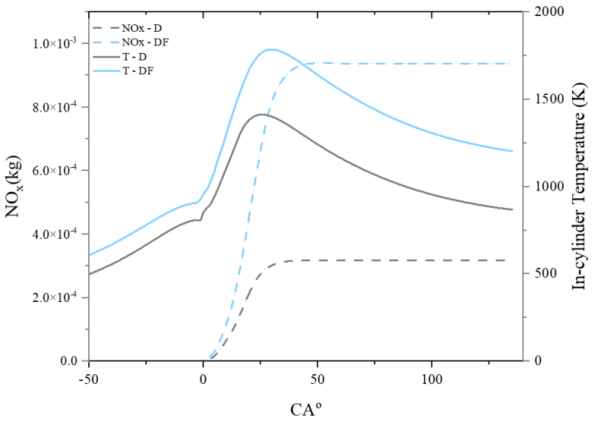

Figure 10. D, DF NOx emissions and temperature in-cylinder.

Fig. 11 shows the in-cylinder hydrogen mass fraction, which illustrates the progression of the hydrogen-air mixture combustion process. At 3ºCA BTDC, the hydrogen-air mixture combustion has not commenced, indicating that the heat release rate (HRR) spike (Fig. 7) is solely attributed to the injected diesel premixed combustion (prepared diesel-air mixture within the region 5–3.7ºCA BTDC). Notably, at 5ºCA ATDC, a considerable hydrogen fraction was noted in the near-wall region; this was attributed to the diesel combustion reactions leading to hydrogen production. The increased temperature in proximity to the diesel jet initiates hydrogen-air mixture combustion. The hydrogen mass fraction is considerably reduced in the period of 20–30ºCA ATDC with the flame front moving, whereas the remaining diesel fuel is burned via a diffusion combustion approach.

4. CONCLUSIONS

This study employed CFD modelling to investigate the impact of hydrogen use in a large marine dual-fuel engine, considering hydrogen port injection and a 20% hydrogen energy fraction. The engine performance and emission parameters were compared for diesel and dual-fuel modes. The developed CFD model was validated using

experimental data for the diesel mode. The study concluded the following.

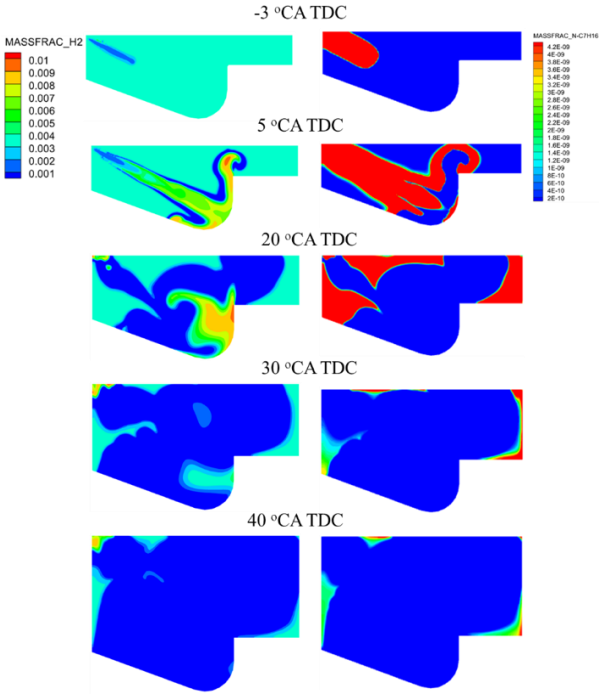

Figure 11. In-cylinder hydrogen and diesel mass fraction variations.

- Maximum in-cylinder pressure reduces from 136 bar to 100 bar due to CR reduction, whereas the CA at maximum pressure retards from 13.5°CA TDC in single fuel to 15.7°CA TDC, for the diesel and dual-fuel modes, respectively.
- The dual-fuel mode exhibits reduced ignition delay and a prolonged diffusion phase in the region 20–30°CA ATDC.
- Indicated thermal efficiency reduces by 2% as heat transfer losses increase under hydrogen operation.
- The hydrogen combustion efficiency was estimated at 93.7%, which indicates that measures to reduce unburnt hydrogen must be further investigated.
- NO_x emissions at the dual fuel mode increased by 260% due to higher in-cylinder temperature.
- The HRR analysis indicated that the premixed hydrogen combustion took place along the diesel diffusion combustion in the range 5–40°CA ATDC.

Future studies could focus on the optimisation of engine settings to accommodate contradicting effects and higher hydrogen energy fractions while maintaining knock-free conditions, minimising unburnt hydrogen, and reducing NO_x emissions, thereby simultaneously providing efficiency improvement and emissions reduction.

FUNDING STATEMENT

The study was carried out in the framework of the AUTOSHIP project (AUTOSHIP, 2022), which is funded by the European Union's Horizon 2020 research and innovation programme under agreement No 815012.

ACKNOWLEDGMENTS

The authors greatly acknowledge the funding from DNV AS and RCCL for the MSRC establishment and operation. The opinions expressed herein are those of the authors and should not be construed to reflect the views of EU, DNV AS and RCCL.

REFERENCES

[1] L. M. Wong, "Hydrogen as marine fuel–feasibility, prospects, and challenges," 2023.

[2] P. Karvounis, J. L. Dantas, C. Tsoumpris, and G. Theotokatos, "Ship Power Plant Decarbonisation Using Hybrid Systems and Ammonia Fuel—A Techno-Economic–Environmental Analysis," Journal of Marine Science and Engineering, vol. 10, no. 11, p. 1675, 2022.

[3] P. Karvounis, C. Tsoumpris, E. Boulougouris, and G. Theotokatos, "Recent advances for sustainable and safe marine engines operation with alternative fuels," Frontiers in Mechanical Engineering, vol. 8, 2022.

[4] P. Dimitriou and T. Tsujimura, "A review of hydrogen as a compression ignition engine fuel," International Journal of Hydrogen Energy, vol. 42, no. 38, pp. 24470-24486, 2017.

[5] J. Gao, X. Wang, P. Song, G. Tian, and C. Ma, "Review of the backfire occurrences and control strategies for port hydrogen injection internal combustion engines," Fuel, vol. 307, p. 121553, 2022.

[6] V. Kumar, D. Gupta, and N. Kumar, "Hydrogen use in internal combustion engine: A review," International Journal of Advanced Culture Technology, vol. 3, no. 2, pp. 87-99, 2015.

[7] A. Ritari, J. Huotari, and K. Tammi, "Marine vessel powertrain design optimization: Multiperiod modeling considering retrofits and alternative fuels," Proceedings of the Institution of Mechanical Engineers, Part M: Journal of Engineering for the Maritime Environment, p. 14750902221145747, 2023.

[8] S. Stoumpos, G. Theotokatos, E. Boulougouris, D. Vassalos, I. Lazakis, and G. Livanos, "Marine dual fuel engine modelling and parametric investigation of engine settings effect on performance-emissions trade-offs," Ocean Engineering, vol. 157, pp. 376-386, 2018.

[9] S. Verhelst and T. Wallner, "Hydrogen-fueled internal combustion engines," Progress in Energy and Combustion Science, vol. 35, no. 6, pp. 490-527, 2009.

[10] N. Castro, M. Toledo, and G. Amador, "An experimental investigation of the performance and emissions of a hydrogen-diesel dual fuel compression ignition internal combustion engine," Applied Thermal Engineering, vol. 156, pp. 660-667, 2019.

[11] P. Dimitriou and T. Tsujimura, "A review of hydrogen as a compression ignition engine fuel," International Journal of Hydrogen Energy, vol. 42, no. 38, pp. 24470-24486, 2017.
[12] "San Diego Mech, 2006," [Online]. Available: http://www.mae.ucsd.edu/combustion/cermech-21.
[13] L. M. Ricart, R. D. Reitz, and J. E. Dec, "Comparisons of diesel spray liquid penetration and vapor fuel distributions with in-cylinder optical measurements," J Eng Gas Turb Power, vol. 122, no. 4, pp. 588–95, 2000.
[14] Z. Y. Han, Z. Xu, and N. Trigui, "Spray/wall interaction models for multidimensional engine simulation," Int J Eng Res, vol. 1, no. 1, pp. 127–46, 2000.
[15] N. Nordin, "Complex chemistry modeling of diesel spray combustion," Ph.D. thesis, Chalmers University, 2001.
[16] A. M. Mellor, J. P. Mello, K. P. Duffy, W. L. Easley, and J. C. Faulkner, "Skeletal Mechanism for NOx Chemistry in Diesel Engines," SAE transactions, pp. 786-801, 1998.
[17] A. Rahimi, E. Fatehifar, and R. K. Saray, "Development of an optimized chemical kinetic mechanism for homogeneous charge compression ignition combustion of a fuel blend of n-heptane and natural gas using a genetic algorithm," Proceedings of the Institution of Mechanical Engineers, Part D: Journal of Automobile Engineering, vol. 224, no. 9, pp. 1141-1159, 2010.
[18] M. Dadashzadeh, S. Kashkarov, D. Makarov, and V. Molkov, "Risk assessment methodology for onboard hydrogen storage," International Journal of Hydrogen Energy, vol. 43, no. 12, pp. 6462-6475, 2018.